Wetting in the binary Gaussian core model

2002 J. Phys.: Condens. Matter 14 1131

(http://iopscience.iop.org/0953-8984/14/6/302)

INSTITUTE OF PHYSICS PUBLISHING JOURNAL OF PHYSICS: CONDENSED MATTER

J. Phys.: Condens. Matter **14** (2002) 1131–1141 PII: S0953-8984(02)30083-3

Wetting in the binary Gaussian core model

A J Archer and R Evans

H H Wills Physics Laboratory, University of Bristol, Bristol BS8 1TL, UK

Received 26 October 2001
Published 1 February 2002
Online at stacks.iop.org/JPhysCM/14/1131

Abstract

Using a simple mean-field density functional approach we investigate the adsorption of a binary fluid mixture of repulsive Gaussian core particles at a repulsive planar wall. For certain choices of wall–fluid potential we find a first-order wetting transition, and the accompanying pre-wetting line, whereby the fluid phase rich in the larger species completely wets the interface between the wall and the fluid phase rich in the smaller species. We show that in the complete wetting regime the film thickness diverges as $l \sim -l_0 \ln(x - x_{\rm coex})$, where $(x - x_{\rm coex})$ is the deviation in concentration x of the smaller species from the bulk binodal, for all the (short-ranged) wall potentials that we have considered but the amplitude l_0 depends on the precise details of these potentials.

1. Introduction

Recently there has been much interest in the statistical mechanics of soft-core particles [1]. A particularly simple example of a soft-core fluid is the Gaussian core model (GCM) [2] where the particles interact via a repulsive Gaussian pair potential. A Gaussian serves as a good approximation for the effective interaction between the centres of mass of two polymer chains in an athermal solvent[1] [1, 4–7]. At high densities the equilibrium pair structure of the GCM is described well by a simple random-phase approximation and the thermodynamics by a mean-field equation of state [1, 7–9]. The reason the GCM behaves as a 'mean-field fluid' is that as the density, ρ, increases, the mean interparticle separation $\rho^{-1/3} \ll R$, the size of the particles, and in the limit $\rho R^3 \to \infty$ a central particle interacts with a very large number of neighbours—the classic mean-field situation. In an earlier paper [10] we investigated the bulk phase behaviour of a binary mixture of repulsive Gaussian core particles using the simple mean-field approach suggested in [7]. For certain choices of energy and size parameters the binary mixture exhibits fluid–fluid demixing. By constructing the density functional which generates the random-phase approximation for the pair direct correlation functions $c_{ij}^{(2)}(r)$ of the bulk mixture, we determined the Fisher–Widom (FW) line [11] which denotes the line in the bulk phase diagram where the asymptotic decay of the total pair correlation functions $h_{ij}(r)$ crosses over from exponentially damped oscillatory form to monotonic decay. The FW

[1] A Gaussian effective potential for polymers was first proposed in [3].

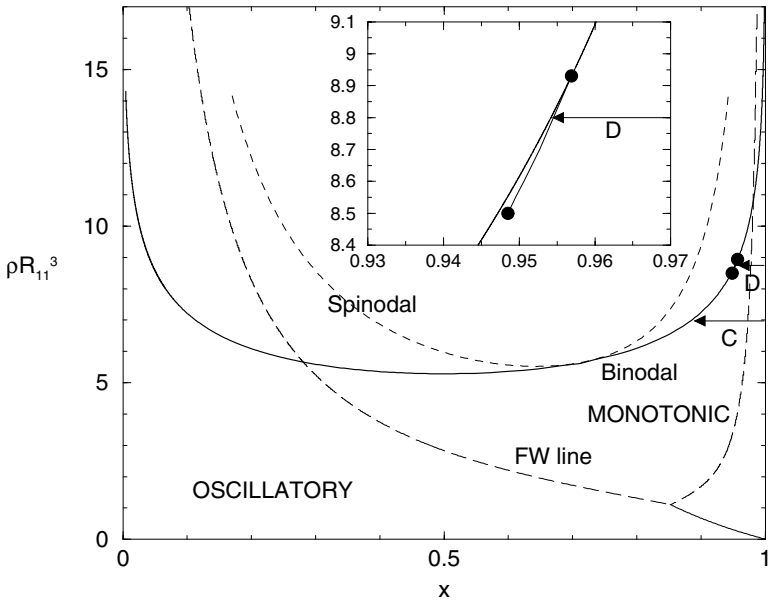

Figure 1. The phase diagram for a mixture of Gaussian particles, equivalent to a mixture of two polymers with length ratio 2:1. ρ is the total density and x is the concentration of the smaller species 2. The dashed curve denotes the FW line where the asymptotic decay of the bulk pairwise correlation functions crosses over from oscillatory to monotonic. The solid curve in the bottom right corner denotes a line of crossover from asymptotic oscillatory decay with a certain wavelength to oscillatory decay but with a different wavelength [10]. The inset shows a magnification of the pre-wetting line, meeting the binodal (solid curve) tangentially at the wetting point, for a wall potential given by equation (8) with $\lambda/R_{11} = 1$. The lower point denotes the pre-wetting critical point. The path in the phase diagram marked C is at fixed $\rho R_{11}^3 = 7.0$ along which the density profiles in figure 3 are calculated. The path marked D is at fixed $\rho R_{11}^3 = 8.8$ along which the profiles in figure 2 are calculated. This path intersects the pre-wetting line.

line has two branches. One intersects the binodal on the side rich in species 1 and the other intersects the binodal on the side rich in species 2 [10]; a specific example is shown here in figure 1. We also found a new line, analogous to the FW line, but now denoting the locus of crossover in the asymptotic decay of the pair correlation functions from damped oscillatory with a certain wavelength to damped oscillatory with a different wavelength. This is also illustrated in figure 1. The same density functional was used to investigate the one-body density profiles $\rho_1(z)$ and $\rho_2(z)$, of species 1 and 2 at the free interface between coexisting fluid phases. For certain states removed from the critical point, $\rho_1(z)$ and $\rho_2(z)$ exhibit damped oscillations on both sides of the interface [10]. The occurrence of the oscillatory profiles was accounted for in terms of general arguments [12] for the asymptotic decay of bulk pairwise correlations; the onset of oscillations is directly linked to the location of the FW line.

This paper is concerned with the adsorption of the binary mixture of Gaussian particles, treated within the same density functional approximation, at a purely repulsive planar wall. We show that for certain choices of wall–fluid potentials, a first-order wetting transition occurs from partial to complete wetting of the interface between the wall and the fluid phase rich in species 2 by the fluid phase rich in species 1. The transition is induced by decreasing the total density ρ of the bulk mixture. Within the complete wetting regime the thickness of the wetting film diverges logarithmically with $(x - x_{\mathrm{coex}})$, where x denotes the concentration of species 2 and x_{coex} its value at bulk coexistence, for all the (short-ranged) wall–fluid potentials that we

investigate. However, the length scale associated with the film growth depends sensitively on the details of these potentials. We also find evidence for a critical wetting transition when the decay length of the wall–fluid potential is particularly short.

2. The model mixture and choice of wall–fluid potentials

The GCM binary mixture is specified by the pair potentials between particle species i and j. These are given by the Gaussian form

$$v_{ij}(r) = \epsilon_{ij} \exp(-r^2/R_{ij}^2) \tag{1}$$

where $\epsilon_{ij} > 0$ denotes the energy and R_{ij}, which is approximately the radius of gyration of the polymer, determines the range of the ij interaction; $1 \leqslant i, j \leqslant 2$. We employ a simple mean-field form for the intrinsic Helmholtz free-energy functional of the inhomogeneous mixture:

$$\mathcal{F}[\{\rho_i\}] = \mathcal{F}_{\mathrm{id}}[\{\rho_i\}] + \tfrac{1}{2} \sum_{ij} \int \mathrm{d}\boldsymbol{r}_1 \int \mathrm{d}\boldsymbol{r}_2 \, \rho_i(\boldsymbol{r}_1)\rho_j(\boldsymbol{r}_2)v_{ij}(|\boldsymbol{r}_1 - \boldsymbol{r}_2|) \tag{2}$$

where $\rho_i(\boldsymbol{r})$ is the average one-body density of species i and $\mathcal{F}_{\mathrm{id}}$ is the ideal-gas part of the free-energy functional. As described in [10], the functional defined by equation (2) generates the random-phase approximation for the pair direct correlation functions: $c_{ij}^{(2)}(\boldsymbol{r}_1, \boldsymbol{r}_2) = c_{ij}^{(2)}(|\boldsymbol{r}_1 - \boldsymbol{r}_2|) = -\beta v_{ij}(|\boldsymbol{r}_1 - \boldsymbol{r}_2|)$, for all inhomogeneities. $\beta = (k_{\mathrm{B}}T)^{-1}$ is the inverse temperature. In the present study we work with the grand potential functional

$$\Omega_V[\{\rho_i\}] = \mathcal{F}[\{\rho_i\}] - \sum_i \int \mathrm{d}\boldsymbol{r} \, [\mu_i - V_i(\boldsymbol{r})]\rho_i(\boldsymbol{r}) \tag{3}$$

where $V_i(\boldsymbol{r})$, $i = 1, 2$, is the external potential acting on species i and μ_i is the chemical potential of that species. An obvious choice of wall–fluid potential is a Gaussian wall with a form analogous to (1):

$$\beta V_i(z) = \begin{cases} \infty & z \leqslant 0 \\ A_i \exp[-(z/R_{ii})^2] & z > 0 \end{cases} \tag{4}$$

where z is the distance from the wall and $A_i > 0$ is an amplitude and we investigated the wetting behaviour of such a model system. Recall that complete wetting by a liquid in a typical one-component fluid may occur at an attractive wall when the bulk gas phase is close to coexistence. Then a film of the liquid phase is adsorbed at the wall whose thickness diverges on approaching coexistence [13][2]. For the GCM binary fluid we sought wetting at the wall by one of the demixed fluid phases. More specifically, the bulk fluid phase was chosen to be that rich in species 2, the smaller particle, (see figure 1) and we sought complete wetting by the fluid phase rich in species 1 by calculating the density profiles $\rho_i(z)$ and adsorption

$$\Gamma_i = \int_0^\infty \mathrm{d}z \, (\rho_i(z) - \rho_i^b) \tag{5}$$

where $\rho_i^b = \rho_i(\infty)$ is the bulk density of species i, on paths corresponding to decreasing x towards x_{coex} (the bulk binodal point) at fixed total density ρ. The profiles are obtained by minimizing the functional (3). With the wall potential given by (4) and amplitude ratios A_2/A_1 which are not far removed from unity, one does not find a transition to complete wetting.

[2] A first-order wetting transition and the accompanying pre-wetting were first obtained by Cahn and by Ebner and Saam in 1977.

However, if one chooses the wall potentials to be of the same Gaussian form, but now with the same decay length λ for both species:

$$\beta V_i(z) = \begin{cases} \infty & z \leqslant 0 \\ A_i \exp[-(z/\lambda)^2] & z > 0 \end{cases} \tag{6}$$

one does find a transition to complete wetting. By making the decay length of the wall–fluid potential the same for both species, one has set the decay length measured on the scale of the smaller of the two species of particles to be longer ranged. The result is an effective attraction between the wall and the larger of the two species which ensures that the smaller species of particles is depleted more strongly from the wall than is the larger. This attraction is in spite of the fact that all the intrinsic particle–particle and wall–particle potentials are repulsive. (Note that although the potentials of equation (4) also generate an effective attraction, this appears to be insufficiently strong to drive the transition.) As a consequence of this attraction, one finds that if the bulk fluid is a phase poor in the larger species, but is near to phase separation, then a wetting film of the coexisting phase, rich in the larger particles, may grow on the wall provided ρ is sufficiently low. Complete wetting is not limited to this particular form of the wall potential. For example, an exponentially decaying wall potential of the form

$$\beta V_i(z) = \begin{cases} \infty & z \leqslant 0 \\ A_i \exp[-z/\lambda] & z > 0 \end{cases} \tag{7}$$

also yields complete wetting. The effective attraction has the same origin as for equation (6).

The studies of Louis *et al* [5, 7] have considered a wall–fluid potential of the form $\beta V(z) = \exp(-z/R)/(z/R)$ for the one-component Gaussian core fluid. This form was motivated by the effective wall potentials obtained from inverting Monte Carlo simulation density profiles of self-avoiding-walk polymers at a hard wall, i.e. the density profile of the Gaussian core fluid at a wall potential of the form $\beta V(z) = \exp(-z/R)/(z/R)$ mimics the polymer centre of mass profile at a hard wall. The obvious generalization to the two-component fluid is to set $\beta V_i(z) = \exp(-z/R_{ii})/(z/R_{ii})$. With this choice of wall potential one does not observe complete wetting; the situation is the same as for the Gaussian wall potential of equation (4). Not surprisingly, if one chooses the wall potentials to be of the same form but with both having the same decay length λ:

$$\beta V_i(z) = \begin{cases} \infty & z \leqslant 0 \\ A_i \exp[-z/\lambda]/[z/\lambda] & z > 0 \end{cases} \tag{8}$$

with $A_i \propto R_{ii}$, then one observes complete wetting for sufficiently low ρ, approaching the bulk critical (consolute) point. For those models where complete wetting occurs, one finds that as one moves up the binodal, away from the critical point, there is a 'wetting point', above which partial wetting occurs; one finds a thin layer, at most two particle diameters thick, adsorbed at the wall. The location of the wetting point on the binodal is dependent on the details of the wall potential. As the transition is (usually) first order there is a pre-wetting line descending to lower ρ from the wetting point. This curve is a tangent to the binodal at the wetting point, and ends in a critical point away from the binodal; see the inset to figure 1. The pre-wetting line is a line of first-order surface phase transitions [13]. For a path in the phase diagram intersecting the pre-wetting line, the film thickness grows very slowly until the pre-wetting transition is reached, where there is a jump in the film thickness. Inside the pre-wetting line the wetting film thickness increases and finally diverges at the binodal. For a path which lies below the pre-wetting critical point, the film thickness increases continuously; there is no jump.

3. Results of calculations

3.1. First-order wetting transition

We illustrate the wetting characteristics for a particular choice of the parameters specifying the binary GCM and for a given choice of the parameters specifying the wall potential (8). Following [7, 10] we chose the pair potential parameters $\epsilon_{11} = \epsilon_{22} = 2k_BT$, $\epsilon_{12}/\epsilon_{11} = 0.944$, $R_{22}/R_{11} = 0.665$ and $R_{12}/R_{11} = 0.849$, which is equivalent to a mixture of two polymers with length ratio 2:1. This binary mixture demixes at sufficiently high total densities, $\rho = \rho_1 + \rho_2$, with a lower critical point at $(x_c, \rho_c R_{11}^3) = (0.70, 5.6)$ (see figure 1), where x is the concentration of species 2, the smaller particles [10]. Figure 1 is a typical binary GCM phase diagram. We have marked on it the wetting point and the pre-wetting line calculated for the wall potential given by equation (8), with $\lambda/R_{11} = 1$, and amplitudes $A_1 = 1$ and $A_2 = R_{22}/R_{11} = 0.665$. The wetting point is at $(x, \rho R_{11}^3) = (0.957, 8.93)$. Descending from the wetting point is the pre-wetting line ending in a critical point at $(x, \rho R_{11}^3) = (0.949, 8.50)$. This line is very short (in ρ) and lies very close to the binodal. The wetting point and the pre-wetting line are determined by analysing the density profiles and the adsorption Γ_1; the latter exhibits a discontinuous jump at the pre-wetting transition.

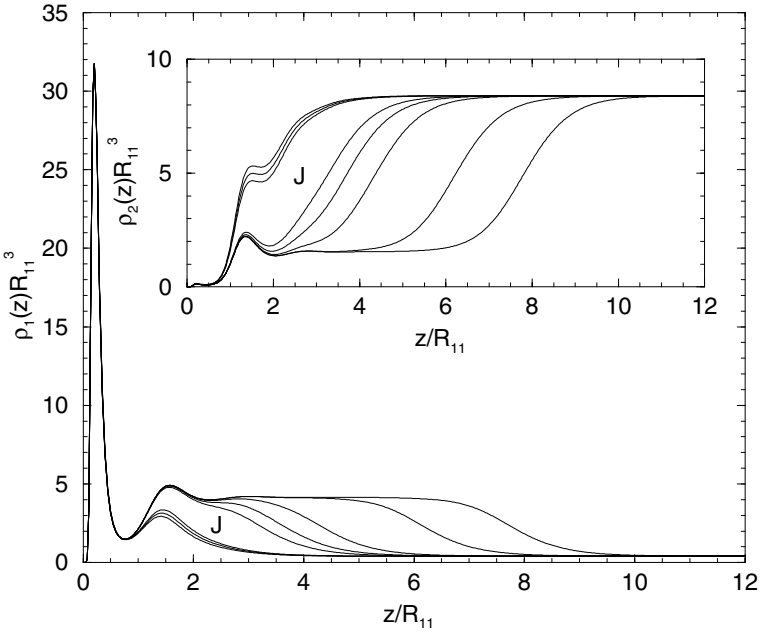

Figure 2. The density profiles of species 1, the larger particles, adsorbed at a wall with external potential given by equation (8) with $\lambda/R_{11} = 1$, calculated along a path of constant total density, $\rho R_{11}^3 = 8.8$, i.e. path D in figure 1 (from left to right the profiles refer to $x = 0.955$, 0.9547, 0.9546, 0.9545, 0.9544, 0.9543, 0.9542 and 0.95419, where x is the concentration of species 2. $x_{\text{coex}} = 0.954\,184\,31$). The thickness of the adsorbed film increases slowly as x decreases until the pre-wetting transition is reached, when there is a jump between $x = 0.9546$ and 0.9545 (marked J) in the profile, and then the thickness of the adsorbed film increases continuously as $x \to x_{\text{coex}}^+$, indicating complete wetting. The inset shows the density profiles of species 2 for the same values of x.

Figure 2 displays some typical density profiles for states approaching the binodal, along path D in figure 1, at a constant bulk density $\rho R_{11}^3 = 8.8$ intersecting the pre-wetting line, and

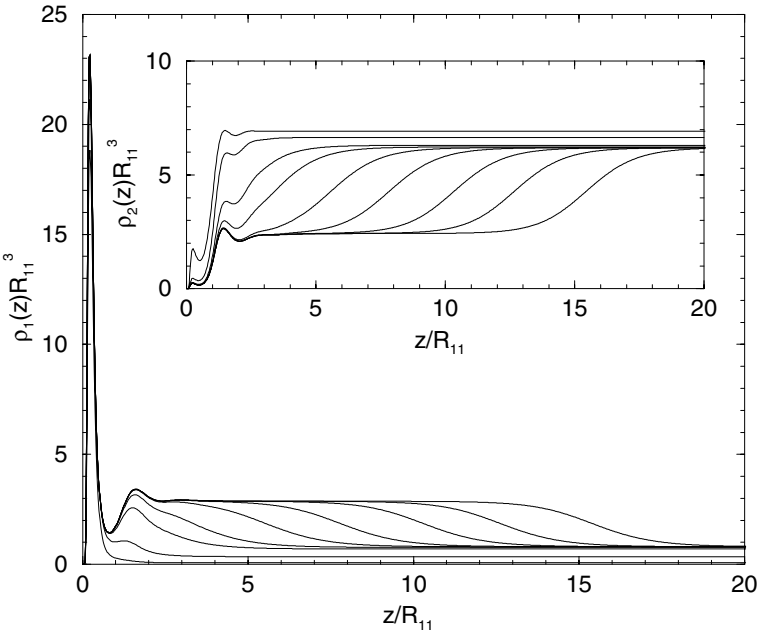

Figure 3. The density profiles of species 1, the larger particles, adsorbed at a wall with external potential given by equation (8) with $\lambda/R_{11} = 1$, calculated along a path of constant total density, $\rho R_{11}^3 = 7.0$, i.e. path C in figure 1 (from left to right the profiles refer to $x = 0.99, 0.95, 0.9, 0.89, 0.886, 0.8855, 0.885\,446, 0.885\,442$ and $0.885\,4416$, where x is the concentration of species 2. $x_{\rm coex} = 0.885\,441\,572$). The thickness of the adsorbed film increases continuously as $x \to x_{\rm coex}^+$, indicating complete wetting. The inset shows the density profiles of species 2 for the same values of x. Note that species 2 is depleted from the region adjoining the wall.

figure 3 displays some typical density profiles for states along path C in figure 1, at a constant bulk density $\rho R_{11}^3 = 7.0$. Since this lower density lies below that of the pre-wetting critical point, the wetting film grows continuously as x is decreased towards $x_{\rm coex}$. In figure 4(a) Γ_1, the adsorption of species 1, corresponding to the density profiles in figure 3, is plotted against the logarithm of the deviation $|x - x_{\rm coex}|$, from coexistence. In the limit $x \to x_{\rm coex}^+$, Γ_1 as defined by equation (5), is proportional to the thickness l of the wetting film, i.e. $\Gamma_1 \sim l(\rho_1^{b,A} - \rho_1^{b,B})$, where $\rho_1^{b,A}$ is the bulk coexisting density of species 1 in phase A, rich in species 1, and $\rho_1^{b,B}$ is the same quantity in phase B, poor in species 1. Γ_1, and therefore l, increase linearly with $-\ln(x - x_{\rm coex})$.

In figure 4(b) Γ_1 is plotted along the constant-density path $\rho R_{11}^3 = 8.8$ (path D in figure 1), corresponding to the density profiles in figure 2, which intersects the pre-wetting line. The jump in Γ_1 occurs at the intersection with the pre-wetting line. As $x \to x_{\rm coex}^+$, Γ_1 and l diverge logarithmically.

These results, along with those for several other choices of potential parameters, point to a classic first-order wetting scenario. The general trend is: the larger the range λ in equation (8), the further the wetting point is from the consolute point. Reducing λ shifts the wetting point towards the consolute point and for sufficiently small values it appears that there can be a crossover to a critical wetting transition. For example, when $\lambda/R_{11} = 0.125$, and amplitudes $A_1 = 1$ and $A_2 = R_{22}/R_{11} = 0.665$, the wetting point moves well below that for $\lambda/R_{11} = 1.0$, to $(x, \rho R_{11}^3) = (0.88, 6.9)$, and there is no indication of a pre-wetting transition. The adsorption Γ_1 appears to diverge continuously (as $-\ln(\rho - \rho_{\rm w})$, where $\rho_{\rm w}$ is the value

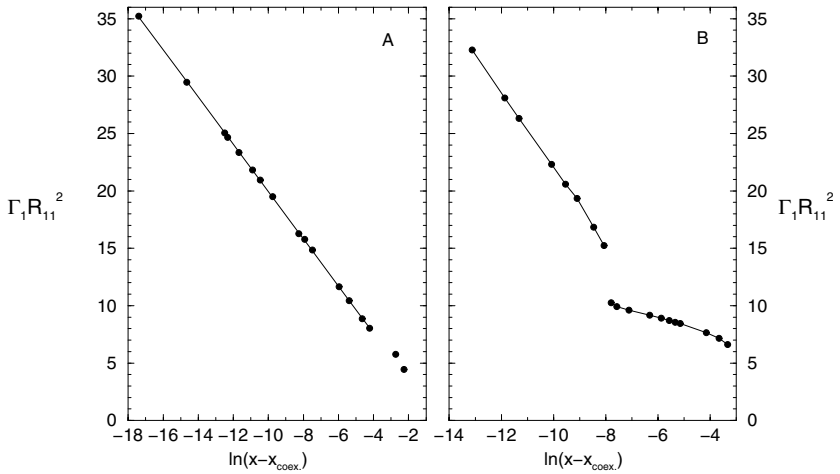

Figure 4. Plots of the adsorption of species 1, Γ_1, at a wall with external potential given by equation (8) with $\lambda/R_{11} = 1$, along two paths of constant total density as a function of the logarithm of the deviation from bulk coexistence, $\ln(x - x_{\rm coex})$. Panel (a) refers to the path $\rho R_{11}^3 = 7.0$, labelled C in figure 1, corresponding to the density profiles in figure 3, which lies below the pre-wetting critical point. Panel (b) refers to the path $\rho R_{11}^3 = 8.8$, labelled D in figure 1, corresponding to the density profiles in figure 2, which intersects the pre-wetting line. The jump in Γ_1 occurs at the intersection. On approaching the binodal, Γ_1 increases linearly with $-\ln(x - x_{\rm coex})$ in both (a) and (b).

of the total density at the wetting transition) as we reduce ρ along the binodal. Further work is required to determine how crossover to critical wetting depends on λ and whether other choices of wall–fluid potential will also lead to critical wetting. Note that crossover to critical wetting with decreasing wall decay length was observed in a generalization of the Sullivan [14] model for a one-component fluid with Yukawa fluid–fluid attraction and exponential wall–fluid attraction [15, 16].

3.2. Thickness of the wetting film

In this subsection we focus on the details of how the thickness l of the wetting film diverges for different choices of wall–fluid potentials. Recall that in the mean-field description, as used in the present study, of wetting for a typical one-component fluid whose interparticle potential is short ranged (potential with finite support, Yukawa, exponential or faster decay), l diverges as $-l_0 \ln \Delta\mu$, where $\Delta\mu = (\mu_{\rm coex} - \mu)$ is the difference in chemical potential from bulk coexistence, provided the wall–fluid potential is also short ranged [13]. The prefactor l_0, i.e. the length scale determining the logarithmic growth, depends in a subtle way on the relative ranges of the wall–fluid and fluid–fluid interparticle potentials. If the former decays exponentially with distance from the wall, one must compare the decay length with $\xi_{\rm w}$, the bulk correlation length of the (liquid) phase which is wetting [13, 16]. The amplitude l_0 will be determined by which length is longer. On the other hand, for Gaussian wall–fluid attraction or for a wall–fluid potential with finite support, one expects the only relevant length scale to be $\xi_{\rm w}$. How does this phenomenology carry over to the present situation of the binary GCM near a wall?

We begin by noting that for all models where we find complete wetting, the calculated adsorption Γ_1 and film thickness l diverge as $-\ln(x - x_{\rm coex})$. For the case of Gaussian wall–fluid

potentials, equation (6), we find that regardless of the wall decay length λ, $l \sim -\xi_w \ln(x - x_{coex})$, i.e. the amplitude is ξ_w, the bulk correlation length in phase A, rich in species 1, which is wetting the wall–phase B interface. It is important to define the bulk correlation length ξ of a binary mixture. This is the exponential decay length describing the (common) asymptotic decay of the three partial pairwise total correlation functions $h_{ij}(r)$. ξ can be obtained from the poles of the Fourier transform of $h_{ij}(r)$ [12] (a more detailed description of the calculation of poles in the GCM can be found in [10]). In Fourier space the Ornstein–Zernike equations for $h_{ij}(r)$ are $\hat{h}_{ij}(q) = N_{ij}(q)/D(q)$, where $\hat{h}_{ij}(q)$ is the three-dimensional Fourier transform of $h_{ij}(r)$ and $N_{ij}(q)$ and $D(q)$ are linear combinations of the (Fourier transformed) pairwise direct correlation functions $c_{ij}^{(2)}(r)$. The poles occur when $D(q) = 0$, and therefore all three $\hat{h}_{ij}(q)$ have the same set of poles: $q_n = \pm\alpha_1 + i\alpha_0$. It is the pole with the smallest imaginary part α_0 that dominates the decay of $h_{ij}(r)$ as $r \to \infty$ and it is this pole that determines the bulk correlation length: $\xi = 1/\alpha_0$. For the path labelled C in figure 1, the coexisting (wetting) phase A is at $(x, \rho R_{11}^3) = (0.458, 5.30)$ for which $\xi_w/R_{11} = 0.905$. Note that the FW line and the other line bottom right in figure 1 are the lines in the bulk phase diagram where crossover occurs between different types of pole dominating the asymptotic decay of $h_{ij}(r)$ [10].

A different scenario occurs for a wall potential of the form given by equation (7). Now we find that the wetting film thickness still grows logarithmically as a function of $(x - x_{coex})$, but the amplitude l_0 is no longer necessarily the bulk correlation length of the wetting phase, ξ_w. Rather we find that $l \sim -l_0 \ln(x - x_{coex})$ where l_0 depends on λ, the wall potential decay length. When $\lambda < \xi_w$, $l_0 = \xi_w$, but when $\lambda > \xi_w$, $l_0 = \lambda$. The variation of l_0 with λ for both types of wall is shown in figure 5.

These results can be accounted for by considering the following expression for the surface excess grand potential per unit area (or effective interface potential) of a GCM subject to a wall potential whose decay is exponential, equation (7):

$$\Omega_s(l; x) = l[\omega^{b,A} - \omega^{b,B}] + \gamma_{w,A} + \gamma_{A,B} + a e^{-l/\xi_w} + b e^{-l/\lambda} + O(e^{-2l/\xi_w}, e^{-2l/\lambda}) \tag{9}$$

where $\gamma_{w,A}$ is the surface tension of the wall–phase A interface, $\gamma_{A,B}$ that of the free A–B interface and a and b are coefficients that depend on ρ [13, 16]. Equation (9) is valid for a complete wetting situation; minimization of Ω_s with respect to l yields the equilibrium film thickness l for a given undersaturation[3] $(x - x_{coex})$. $\omega^{b,B}$ is the grand potential per unit volume in bulk phase B at given chemical potentials μ_1 and μ_2, while $\omega^{b,A}$ is the corresponding quantity in phase A at the same chemical potentials. To lowest order in the chemical potential deviations:

$$[\omega^{b,A} - \omega^{b,B}] \simeq (\rho_1^{b,A} - \rho_1^{b,B})\Delta\mu_1 + (\rho_2^{b,A} - \rho_2^{b,B})\Delta\mu_2 \tag{10}$$

where, as previously, $\rho_i^{b,A}$ denotes the bulk coexisting density of species i in phase A etc. Since $\Delta\mu_i \equiv (\mu_i - \mu_{i,coex}) \propto (x - x_{coex})$, to lowest order, it follows that the first term on the right-hand side of equation (9) is proportional to $(x - x_{coex})$. If $\lambda < \xi_w$, the term in $\exp(-l/\xi_w)$ dominates and minimization yields $l \sim -\xi_w \ln(x - x_{coex})$, whereas if $\lambda > \xi_w$, the other exponential dominates and $l \sim -\lambda \ln(x - x_{coex})$. When the wall potential is a Gaussian, equation (6), the term in $\exp(-l/\lambda)$ is absent from Ω_s and minimization yields $l \sim -\xi_w \ln(x - x_{coex})$ for all λ.

[3] Note that equation (9) is appropriate for fluid states where the wetting phase (A) at bulk coexistence lies on the monotonic side of the FW line. This is the case for path C in figure 1. If the wetting phase lies on the oscillatory side of the FW line, the term in $\exp(-l/\xi_w)$ should be multiplied by a factor of $\cos(\alpha_1 l + \phi)$, where α_1 is the real part of the dominating pole and ϕ is a phase factor—see [17].

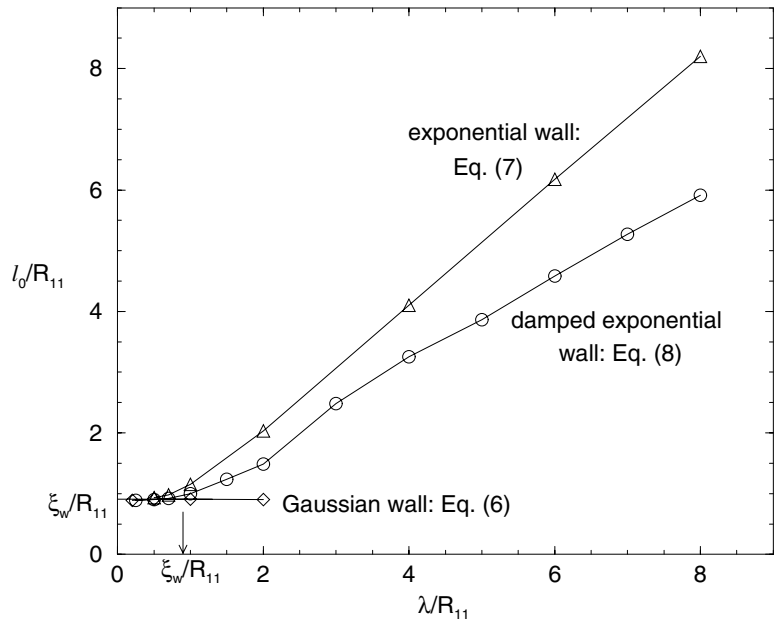

Figure 5. The prefactor l_0 of the wetting film thickness ($l \sim -l_0 \ln(x - x_{\rm coex})$) versus the wall potential decay length λ. In all cases the density profiles were calculated along the constant-density path $\rho R_{11}^3 = 7.0$ (path C in figure 1). For the Gaussian wall ($\Diamond$), $l_0 = \xi_{\rm w}$, the bulk correlation length of the wetting phase, independent of λ. For the exponential wall ($\triangle$), $l_0 = \xi_{\rm w}$ for $\lambda < \xi_{\rm w}$ and $l_0 = \lambda$ for $\lambda > \xi_{\rm w}$. For the wall potential $\beta V_i(z) = A_i \exp(-z/\lambda)/(z/\lambda)$, $z > 0$ ($\bigcirc$), $l_0 = \xi_{\rm w}$ for $\lambda < \xi_{\rm w}$ (see footnote 4) but has a complex variation for $\lambda > \xi_{\rm w}$. The results for the three choices of potential do not appear to depend on the amplitudes A_i.

Equation (9) is not appropriate to the wall potential given by equation (8), i.e. the damped exponential. Although l diverges logarithmically for all choices[4] of λ and $l_0 = \xi_{\rm w}$ for $\lambda < \xi_{\rm w}$, when $\lambda > \xi_{\rm w}$, l_0 is equal to neither $\xi_{\rm w}$ nor λ, but is a monotonically increasing function of λ; see figure 5. For $\lambda/R_{11} \gtrsim 5$, l_0 increases linearly with λ but with the slope < 1. This implies that the relevant term in equation (9) is not of the form $b \exp(-l/\lambda)$. Rather it should be $b' \exp(-l/\lambda')$, where the length $\lambda' \simeq 0.7\lambda$. Whether such a form for $\Omega_s(l; x)$ can be derived by the methods of [16] starting from the full binary mixture density functional, equation (2), remains to be seen.

4. Concluding remarks

We have shown that the binary GCM subject to purely repulsive, short-ranged, wall–fluid potentials can exhibit a first-order wetting transition, with the accompanying pre-wetting, similar to that found in systems where the fluid–fluid and wall–fluid potentials are explicitly attractive. Our results illustrate the ubiquity of wetting transitions and related interfacial phenomena. The wetting transition in the present case is driven by an effective attraction between the wall and the larger species of Gaussian core particle, which arises from the fact that the wall potential is longer ranged on the scale of the smaller particles than on the scale of the larger, leading to strong depletion at the wall of the smaller species. Generating sufficient

[4] We do not include very small values of λ where the wetting point might lie below $\rho R_{11}^3 = 7.0$.

effective attraction between the wall and one of the particle species for a wetting transition to be observed is not only achieved by setting the wall decay length to be the same in both wall potentials. One could achieve sufficient effective attraction between the wall and species 1 by setting the amplitude, A_2 (see equations (6)–(8)), of the potential acting on the smaller species 2 to be much larger than A_1. We also showed that the precise form of the decay of the wall potential determines the amplitude l_0 of the thickness, l, of a wetting film. For an exponentially decaying wall–fluid potential with decay length λ, equation (7), l_0 is determined by the larger of ξ_w, the bulk correlation length in the wetting phase, and λ; i.e. the effective interface potential equation (9) provides an accurate description of the relevant length scales. However, for a wall potential of the form (8), a new length scale may enter which is neither ξ_w nor λ.

Our results are based upon what is arguably the simplest density functional theory, namely the mean-field functional (2), that one might contemplate for any binary fluid mixture. That such a simple theory should predict such rich wetting behaviour is pleasing, but we should enquire how our results might be changed by utilizing more sophisticated functionals. The study of Louis *et al* [7] indicated that for a one-component GCM near a repulsive wall of the type (8), the mean-field functional yields density profiles close to those from a functional which generates the HNC closure of the wall–particle Ornstein–Zernike equation. (Recall that for the bulk structure of the one-component GCM, the HNC closure gives results almost indistinguishable from simulation data [7].) For the binary GCM there are, as yet, no simulation or theoretical results against which we can test those of the present functional. However, for the high-total-density situations that we consider here there are good reasons to expect [10] the random-phase approximation and the functional (2) to be reliable for this soft-core fluid. We speculate that the location of the wetting point might depend sensitively on the details of the free-energy functional but that the gross features of the interfacial phase behaviour should be captured by the simplest treatment.

The theory that we have presented is strictly mean field; capillary-wave fluctuations are omitted in this as well as in other, more refined, density functional approaches. There is a rich phenomenology associated with fluctuations, in particular for systems with short-ranged forces [13, 16, 18]. It would be of some interest to examine fluctuation effects in the present model of a binary mixture, especially for those choices of parameters where a critical wetting transition occurs[5].

Finally, we note that in recent studies of a model colloid–polymer mixture at a hard wall, Brader *et al* [19] found layering transitions at points on the binodal, above the wetting transition point. Although the binary GCM exhibits oscillatory density profiles at the free fluid–fluid interface [10], similar to those found in [19], we do not find any layering transitions in the present model, i.e. the transition from partial to complete wetting is not accompanied by the precursor layering. Layering transitions are associated with many-body terms in the effective one-component Hamiltonian for the colloids [19]. Analogous terms are not expected in the present case.

Acknowledgments

We benefited from helpful discussions with J M Brader, S Dietrich, C N Likos, A O Parry and R Roth. AJA was supported by an EPSRC studentship.

[5] In treatments based on an effective interface potential, it is the dimensionless parameter $\omega = (4\pi\beta\gamma_{A,B}\xi_w^2)^{-1}$, where $\gamma_{A,B}$ is the surface tension, which determines the strength of fluctuation effects [13, 18]. For the present model it might be possible to vary ω over a large range by tuning the parameters of the potentials.

References

[1] Likos C N 2001 *Phys. Rep.* **348** 267 and references therein
[2] Stillinger F H 1976 *J. Chem. Phys.* **65** 3968
see also Stillinger F H and Stillinger D K 1997 *J. Phys. A: Math. Gen.* **244** 358
[3] Flory P J and Krigbaum W 1950 *J. Chem. Phys.* **18** 1086
[4] Dautenhahn J and Hall C K 1994 *Macromolecules* **27** 5399
[5] Louis A A, Bolhuis P G, Hansen J-P and Meijer E J 2000 *Phys. Rev. Lett.* **85** 2522
[6] Bolhuis P G, Louis A A, Hansen J-P and Meijer E J 2001 *J. Chem. Phys.* **114** 4296
[7] Louis A A, Bolhuis P G and Hansen J-P 2000 *Phys. Rev.* E **62** 7961
[8] Lang A, Likos C N, Watzlawek M and Löwen H 2000 *J. Phys.: Condens. Matter* **12** 5087
[9] Likos C N, Lang A, Watzlawek M and Löwen H 2001 *Phys. Rev.* E **63** 031206
[10] Archer A J and Evans R 2001 *Phys. Rev.* E **64** 041501
[11] Fisher M E and Widom B 1969 *J. Chem. Phys.* **50** 3756
[12] Evans R, Leote de Carvalho R J F, Henderson J R and Hoyle D C 1994 *J. Chem. Phys.* **100** 591
[13] See the review by Dietrich S 1988 *Phase Transitions and Critical Phenomena* vol 12, ed C Domb and J L Lebowitz (London: Academic) p 1
Cahn J W 1977 *J. Chem. Phys.* **66** 3667
Ebner C and Saam W F 1977 *Phys. Rev. Lett.* **38** 1486
[14] Sullivan D E 1979 *Phys. Rev.* B **20** 3991
Sullivan D E 1981 *J. Chem. Phys.* **74** 2604
[15] Aukrust T 1987 *PhD Thesis* Institutt for Teoretisk Fysikk, Norges Tekniske Hogskole Trondheim
[16] Aukrust T and Hauge E H 1987 *Physica* A **141** 427
[17] Henderson J R 1994 *Phys. Rev.* E **50** 4836
[18] For a recent review see Parry A O 1996 *J. Phys.: Condens. Matter* **8** 10 761
[19] Brader J M 2001 *PhD Thesis* University of Bristol
Also see Evans R, Brader J M, Roth R, Dijkstra M, Schmidt M and Löwen H 2001 *Phil. Trans. R. Soc.* A **359** 961
Brader J M, Evans R, Schmidt M and Löwen H 2002 *J. Phys.: Condens. Matter* **14** L1